Journal of Power Sources 195 (2010) 5258–5268

Contents lists available at ScienceDirect

Journal of Power Sources

journal homepage: www.elsevier.com/locate/jpowsour

Influence of local porosity and local permeability on the performances of a polymer electrolyte membrane fuel cell

Tilda Akiki[a,b,*], Willy Charon[b,1], Marie-Christine Iltchev[b,1], Gilbert Accary[a,1], Raed Kouta[b,1]

[a] Université Saint Esprit Kaslik, Lebanon
[b] Université de Technologie de Belfort-Montbéliard, FCLAB Institute for Research on Fuel Cell Systems, 90010 Belfort, France

ARTICLE INFO

Article history:
Received 4 December 2009
Received in revised form 5 March 2010
Accepted 8 March 2010
Available online 15 March 2010

Keywords:
Polymer electrolyte membrane fuel cell
Multi-physical interaction
Fuel cell modeling
Performance

ABSTRACT

In the literature, many models and studies focused on the steady-state aspect of fuel cell systems while their dynamic transient behavior is still a wide area of research. In the present paper, we study the effects of mechanical solicitations on the performance of a proton exchange membrane fuel cell as well as the coupling between the physico-chemical phenomena and the mechanical behavior. We first develop a finite element method to analyze the local porosity distribution and the local permeability distribution inside the gas diffusion layer induced by different pressures applied on deformable graphite or steel bipolar plates. Then, a multi-physical approach is carried out, taking into account the chemical phenomena and the effects of the mechanical compression of the fuel cell, more precisely the deformation of the gas diffusion layer, the changes in the physical properties and the mass transfer in the gas diffusion layer. The effects of this varying porosity and permeability fields on the polarization and on the power density curves are reported, and the local current density is also investigated. Unlike other studies, our model accounts for a porosity field that varies locally in order to correctly simulate the effect of an inhomogeneous compression in the cell.

1. Introduction

In the literature, many models have been developed to take into consideration multi-physical phenomena in a fuel cell. Zhou et al. [1–3] developed a sequential approach to study the pressure effects by combining the mechanical and electrochemical phenomena in fuel cells. The pressure causes the deformation of the gas diffusion layer (GDL), and impacts the mass transfer and the electrical contact resistance. The GDL porosity in the PEM (polymer electrolyte membrane) type fuel cell (PEMFC) is also affected by the clamping pressure; however, a global value of the GDL porosity is taken into account (not a local porosity distribution) and the GDL permeability is kept constant. There is an optimal width of the rib of the bipolar plate that gives a small contact resistance and a good porosity of the GDL. At the same time, Zhou et al. studied the impact of the inhomogeneous compression of the GDL on the performance of their fuel cell; the membrane and the catalyst deformation were not taken into account. With a finite elements method, they analyzed the contact pressure, the deformation of the GDL and the porosity distribution. The results showed that a higher clamping force decreases the GDL porosity, which increases the resistance to mass transport and decreases the contact resistance and electric losses. This is how it was found that there is an optimal clamping force that supplies a maximum power density. On the other hand, Zhang et al. [4] proposed two methods for the estimation of the contact resistance between the bipolar plates and the GDL of a PEMFC. The first method is experimental while the second one is numerical based on a finite element method analysis. They deduced that the contact resistance is influenced by the average value of the assembly clamping pressure. From an experimental point of view, Nitta et al. [5] investigated the inhomogeneous compression of the GDL of a PEMFC caused by the channel/rib structure of the flow plate. This study proved that a higher compression improves the GDL conductivity, reduces the contact resistance between the GDL and the electrode and hinders the mass transport by modifying the porosity that is considered homogeneous all through the paper. Fekrazad and Bergman [6] developed a two-dimensional model of the PEMFC in order to study the effect of the changes in the compression force during the assembly of the stack, which modifies the properties of the fuel cell; the model was a steady-state one and the flow was considered laminar. The model evaluated the electric and thermal resistances as well as the permeability by means of experimental data; these properties depend on the clamping pressure and were accounted for in the model, however, the GDL porosity

* Corresponding author at: BP: 446 Jounieh, Lebanon. Tel.: +961 9 600900; fax: +961 9 600901.
E-mail addresses: tildaakiki@usek.edu.lb, tilda.akiki@utbm.fr (T. Akiki), willy.charon@utbm.fr (W. Charon), marie-christine.iltchev@utbm.fr (M.-C. Iltchev), gilbertaccary@usek.edu.lb (G. Accary), raed.kouta@utbm.fr (R. Kouta).
[1] Tel.: +961 9 600900; fax: +961 9 600901.

0378-7753/$ – see front matter © 2010 Elsevier B.V. All rights reserved.
doi:10.1016/j.jpowsour.2010.03.020

Nomenclature

Alphabets

D_{ij}	diffusion coefficient ($m^2\ s^{-1}$)
$drag_{H_2O}$	water drag coefficient
e_v	volumetric deformation
F	Faraday's constant $F = 96{,}487$ ($C\ mol^{-1}$)
i_a	anodic local current density ($A\ m^{-2}$)
$i_{0,a}^{ref}$	anodic exchange current density ($A\ m^{-2}$)
$i_{0,c}^{ref}$	cathodic exchange current density ($A\ m^{-2}$)
i_c	cathodic local current density ($A\ m^{-2}$)
k_e	effective electronic conductivity of electrode ($S\ m^{-1}$)
k_m	ionic conductivity of membrane ($S\ m^{-1}$)
K	permeability
M_{H_2}	hydrogen molar mass ($kg\ mol^{-1}$)
M_{O_2}	oxygen molar mass ($kg\ mol^{-1}$)
M_{H_2O}	water molar mass ($kg\ mol^{-1}$)
N_{O_2}	oxygen mass flux
N_{H_2}	hydrogen mass flux
N_{H_2O}	water mass flux
p	pressure (Pa)
R	gas constant $R = 8314$ ($J\ mol^{-1}\ K^{-1}$)
T	temperature (K)
u	flux velocity ($m\ s^{-1}$)
V_{cell}	operation potential of fuel cell (V)
V_e	potential of electrodes
V_m	potential of membrane

Greek symbols

ε	porosity
ρ	density (kg/m^3)
ω_i	mass fraction of species i
η	dynamic viscosity (Pa s)
η_{act}	activation overpotential (V)
α	transfer coefficient

was kept constant. The study showed in this case the dependency of the fuel-cell power density and the temperature gradients in the membrane on the clamping pressure. Hottinen et al. [7] evaluated the inhomogeneous compression of the GDL and studied the effect on the mass and charge transfers inside the cell. The physical properties of the GDL that are affected by its inhomogeneous compression are: its porosity, its permeability, its conductivity and the contact resistance between the GDL and the electrode. The study investigated experimentally these physical properties as a function of the GDL thickness, and the results were then compared to those obtained from a conventional model in which the parameters were kept constant. This study stated that the inhomogeneous compression of the GDL influences the current density distribution because of the variation of the contact resistance between the GDL and the electrode. Sun et al. [8] proposed a 2D model, in a steady-state and isothermal regime in order to study the influence of the GDL properties and of the flow-channels geometry on the rate of the local reaction inside the cathode/catalyst layer of a PEMFC. The study showed that a larger channel facilitates the transport of chemical species but a narrower rib hinders the transport of electrons. Finally, Al-Baghdadi and Al-Janabi [9,10] developed a 3D steady-state, non-isothermal, and single-phase model of a PEMFC. The model takes into account the major transport phenomena in the fuel cell: convection and diffusion. The strength of the algorithm is its precise evaluation of the activation overvoltage; this gives a better prediction of the local current distributions. All the factors, such as the temperature, the pressure, the porosity, the thermal conductivity, the membrane thickness, the potentials, etc. that might influence the fuel cell performance were studied along with their effects on the current density distribution; however, porosity was kept constant. Their model is then developed into a multiphase one that investigates the displacement, the deformation and the stress inside the whole cell due to the changes of temperature and relative humidity.

In this paper, we are interested in PEM type fuel cells often encountered in transportation, with graphite bipolar plates or steel bipolar plates. We aim to show the influence of mechanical compression on multi-physical phenomena that influence the performance and the durability of PEMFCs. Particularly, we emphasize the effects of the GDL porosity on the polarization and on the power density curves; this porosity field is not uniform but varies locally due to the mechanical compression of the fuel cell. We consider three section types for the channels of the bipolar plates that are made of graphite or steel; these bipolar plates are here considered deformable. Hence, we deepen the complex concept of multi-physical coupling between physico-chemical phenomena and the mechanical behavior in order to simulate the real conditions of use of a PEMFC. In particular, the compression of the fuel cell distorts the GDL and affects its physical properties: the contact resistance between the GDL and the bipolar plate varies, porosity also varies locally as well as permeability. Failures in the fuel cell components and a modification of the charge transport might appear, resulting in a change of the fuel cell performance.

In this study, we first develop a finite element method to analyze the local porosity and the local permeability distributions inside the GDL that are induced by different compression forces applied on two types of deformable bipolar plates (graphite and steel ones). This mechanical approach is carried on first in order to study the effect of the bipolar-plate compression, which induces the GDL deformation, hence affecting its porosity and its permeability. Then, a multi-physical approach is carried out, accounting for the chemical phenomena and the effects of mechanical compression of the fuel cell, more precisely the GDL deformation and the changes in its physical properties and of the mass transfer inside it. The effects of these variable porosity and permeability fields on the polarization and on the power density curves are reported, and the local current density is also investigated. Thus, in our model and unlike previously reported studies, we take into account a variable porosity field, not a constant GDL porosity or an average global value

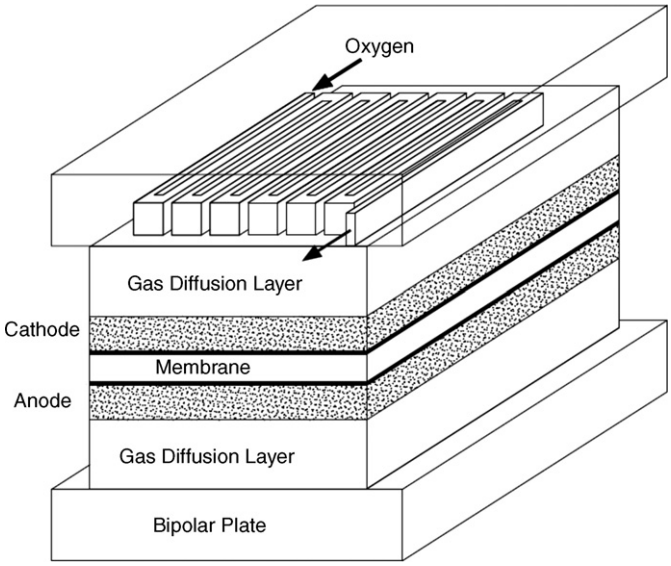

Fig. 1. Modeling elements of a fuel cell.

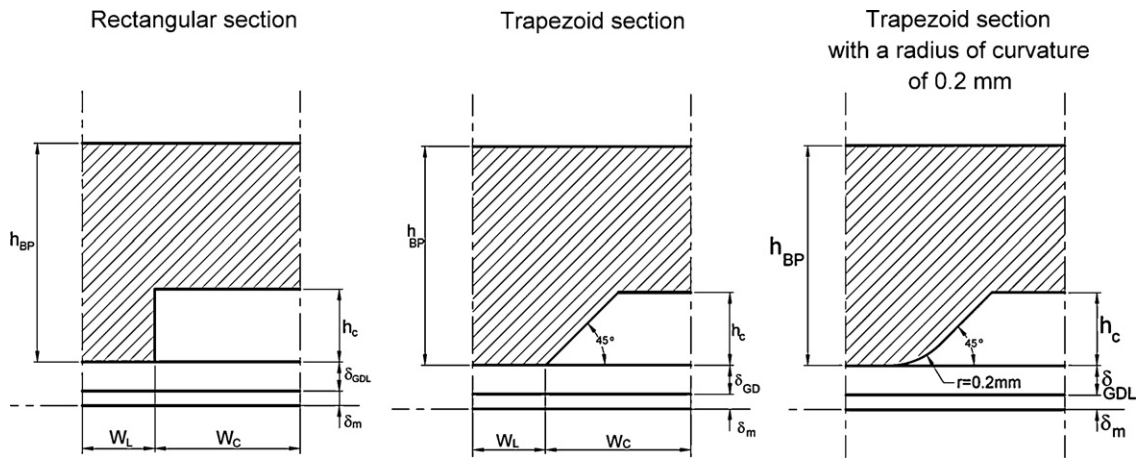

Fig. 2. Different profiles for the ribs of the graphite bipolar plates in contact with the GDL.

of the GDL porosity, in order to correctly simulate the effect of an inhomogeneous compression of the fuel cell.

2. General approach

2.1. Mechanical description of the GDL

Referring to Fig. 1 that shows the modeling elements of a fuel cell, a 2D model consisting in a half-rib and a half-channel from the cathode side of a PEMFC is developed in order to investigate the effects of different compression forces on the GDL deformation. Only a portion of the fuel cell has been considered for computation because of its geometric periodicity. The *X* axis is in the cell thickness direction (vertical direction in Fig. 1), while the *Y* axis denotes the cell width direction (the horizontal one). The bottom surface of the GDL is fixed and the vertical boundaries have symmetry conditions. The physical and geometric properties are listed in Tables 1 and 2 and the initial porosity of GDL is set to 0.75.

Different homogeneous pressures (1 MPa, 5 MPa and 10 MPa) are applied on the bipolar plates for different sections of the channels: a rectangular section of the rib, a trapezoid section, and a trapezoid section of the rib with a 0.2 mm curvature radius (see Figs. 2 and 3). The thickness of the steel bipolar plates is 0.07 mm and their external dimensions are the same as those of the graphite ones.

Hereafter, we present the computation steps required to obtain the porosity field: a finite element analysis is carried on in order to obtain the deformation field in the GDL. Then, the porosity and per-

Table 1
Electro-chemical transport parameters of the fuel cell.

Parameter	Symbol	Value	Unit
Initial porosity of GDL	ε	0.75	-
Electronic conductivity of electrodes	k_e	100	$S\,m^{-1}$
Ionic conductivity of membrane	k_m	17.12	$S\,m^{-1}$
Electrode permeability	K	1.e-13	m^2
Water drag coefficient	$drag_{H_2O}$	3	-
GDL Young modulus		60	MPa
GDL Poisson ratio		0.09	
Graphite bipolar plate: Young modulus		10	GPa
Graphite bipolar plate: Poisson ratio		0.3	
Steel bipolar plate: Young modulus		200	GPa
Steel bipolar plate: Poisson ratio		0.3	

Table 2
Geometric and operation parameters of the fuel cell.

Parameter	Symbol	Value	Unit
Initial hydrogen mass fraction	ω_{H_2}	0.1	-
Initial oxygen mass fraction	ω_{O_2}	0.168	-
Initial water mass fraction	$\omega_{H_2O,c}$	0.2	-
Temperature	T	353	K
Anode pressure	p_a	1.1	atm
Cathode pressure	p_c	1.1	atm
Dynamic viscosity	η	2.1e-5	$m^2\,s^{-1}$
Membrane thickness	δ_m	0.1e-3	m
GDL thickness	δ_{GDL}	0.2e-3	m
Channel width	w_c	1.e-3	m
Rib width	w_1	0.5e-3	m
Channel height	h_c	0.5e-3	m
Bipolar plate height	h_{BP}	1.5e-3	m

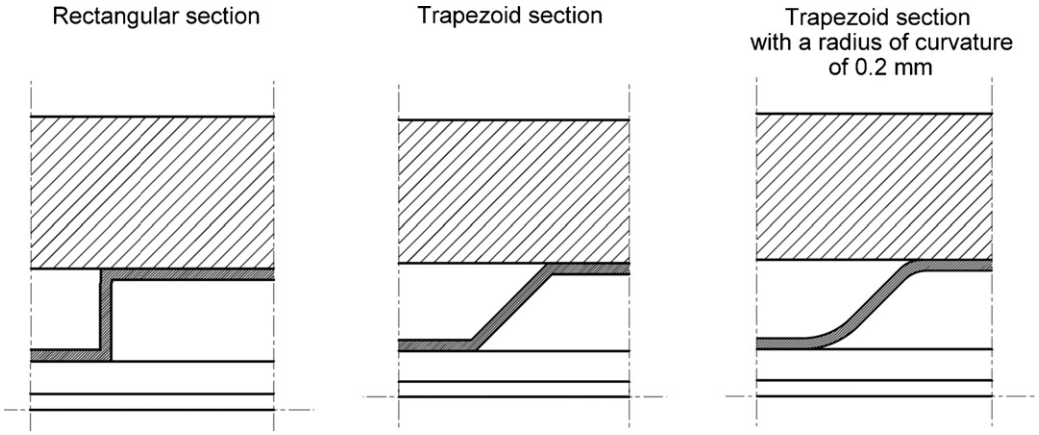

Fig. 3. Different profiles for the ribs of the steel bipolar plates in contact with the GDL.

meability fields are evaluated and introduced in the multi-physical model of the fuel cell in order to obtain the polarization and power density curves.

2.2. Multi-physical approach

In the 2D multi-physical model of the fuel cell, the effects of GDL compression are taken into account, i.e. the deformation of the GDL and the porosity and permeability fields that vary locally. Porosity is also involved in the expressions of the effective diffusion coefficients which, consequently, vary locally too.

We consider a geometry composed of the membrane and the GDL from both the cathode and the anode sides (see Fig. 4). Due to GDL deformation symmetry, we only consider a rib and two half-channels from each side of the rib, and the electrodes and the catalyst layers are considered as internal boundaries in the domain. Given that the reaction rate of the hydrogen oxidation is faster than that of the oxygen reduction, only the deformation of the GDL at the cathode side is modeled; the GDL is compressed under the rib and inflates under the channels. A flux of air (oxygen, nitrogen, and water) is applied at the cathode, the anode is supplied with humidified hydrogen, and a pressure difference exits between the channels (at the left and the right sides of the rib). The following assumptions are made:

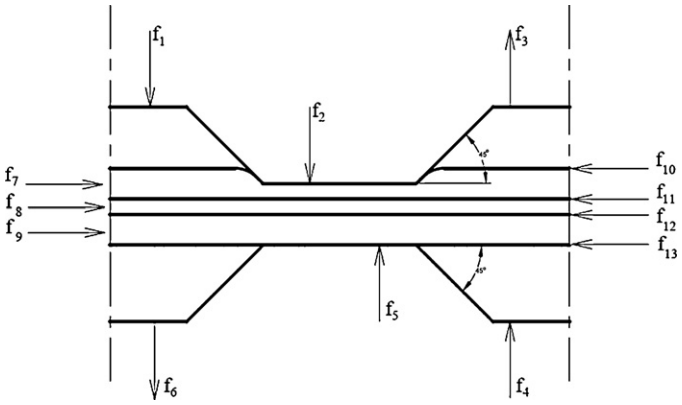

Fig. 4. Boundary conditions of the studied model. f1: Entry of humidified air; water and oxygen; mass fractions and pressures are set. f2: V_{cell}. f3: Exit of humidified air; convective flux at reference pressure. f4: Entry of humidified hydrogen; hydrogen mass fraction and pressure are set. f5: $V = 0$. f6: Exit of humidified hydrogen; convective flux at reference pressure. f7: GDL cathode side. f8: Membrane. f9: GDL anode side. f10: Border GDL-BP cathode side. f11: Cathode border: mass flux and velocity are set. f12: Anode border: mass flux and velocity are set. f13: Border GDL-BP anode side.

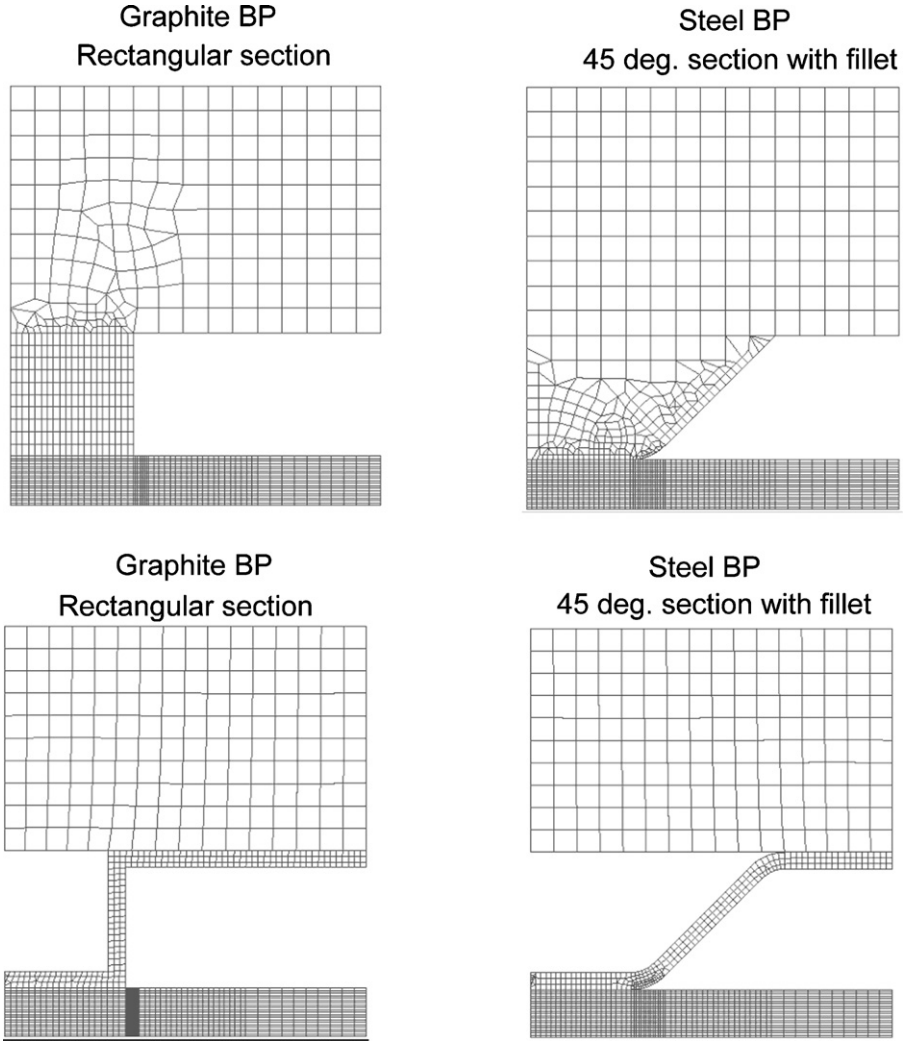

Fig. 5. The finite elements models for different sections of the bipolar plates.

- air and hydrogen are ideal gas mixtures, they are saturated in water vapor,
- the GDL and the catalyst are homogeneous and isotropic,
- the flow is laminar,
- temperature is kept constant,
- water produced from the reduction of oxygen and from water migration from the anode to the cathode is in the liquid phase.

The mechanical compression of the GDL modifies its porosity and, consequently, influences the effective diffusion coefficients and the permeability, which justifies our multi-physical approach of the fuel cell. The interesting point is to see how the compression of the fuel cell influences its power production and its local current density.

The polarization curves, the power density curves, and the local current density are obtained from several simulations in which the fuel cell potential varies from 0 up to 1 V with steps of 0.05 V.

3. Studied models

3.1. Mechanical model for deformation analysis

The objective is to define the deformation of the GDL surface induced by the compression of the bipolar plate that is loaded with a uniform pressure. Since a mechanical modeling of a fuel cell was already done using SAMCEF-Field software for other purposes, the simulation is conducted using this software.

The 3D model consists of two solids obtained by profile extrusion; the first solid is the bipolar plates and represents a half-rib and a half-channel for symmetry reasons, the other one represents the GDL and is in contact with the first solid. Three different geometries of the contact between the bipolar-plate profile and the GDL are studied: a rectangular rib, a trapezoid one, and a trapezoid rib with rounded edges (see Figs. 2 and 3).

In order to study the effect of the deformation of the bipolar plate on the behavior of the GDL, two different materials and their associated geometries are considered for the bipolar plate: the first type is a solid made of graphite and the second one is composed of two steel solids in contact. Fig. 5 represents the finite element modeling of two section types for the above-mentioned materials; the GDL is at the lower part of the sub-figures.

Different pressures (1 MPa, 5 MPa, and 10 MPa) are applied at the top of the bipolar plate, the bottom boundary of the GDL is blocked, as well as the front and rear boundaries of the solids (in the Z direction), and symmetry conditions are applied on the vertical boundaries of both the bipolar plate and the GDL. The model also

Table 3
Diffusion coefficient constants used in Eq. (4).

	O_2–N_2	O_2–H_2O	H_2–H_2O	H_2O–N_2
C_D	0.22	0.282	0.915	0.256
T_{ref}	293.2	308.1	307.1	307.5

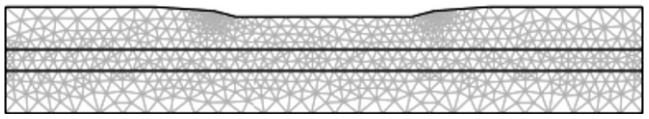

Fig. 6. Example of a mesh for the determination of the polarization and the power density curves of the fuel cell (trapezoid section with a radius of curvature).

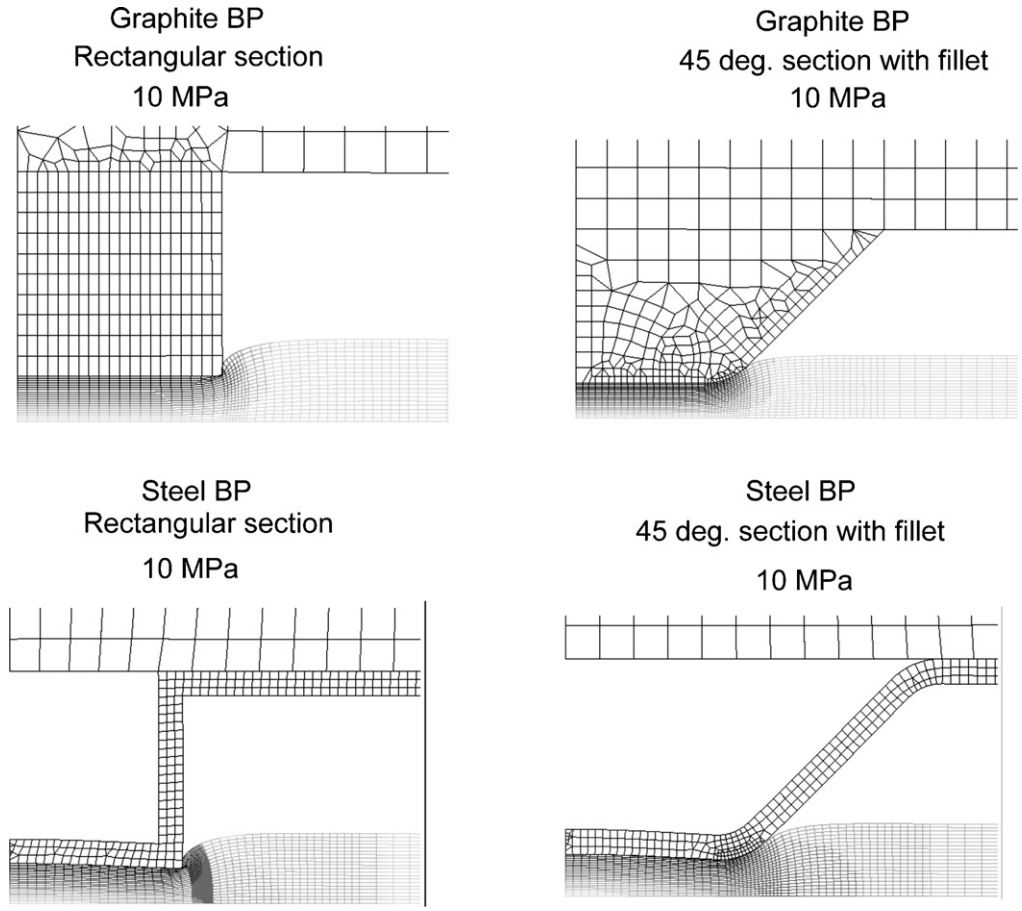

Fig. 7. Mechanical deformations for different sections and materials—10 MPa.

Table 4
Decrease of GDL thickness under the rib of a graphite bipolar plate.

Section of bipolar plate	Pressure (MPa)		
	1	5	10
Rectangular	4.4%	22%	44%
Trapezoid	4.5%	22.7% (Fig. 8, upper figure)	45%
Trapezoid with a 0.2 mm curvature radius	4.9%	23% (Fig. 8, lower figure)	44.4%

takes into account the nature of the mechanical contact between the bipolar plate and the GDL.

The mesh consists of one row (in the Z direction) of 3D hexa- and penta-type elements; the mesh is refined in the contact zones and in the zones that are likely to become in contact after deformation. This deformation is evaluated from the vertical displacements of the nodes that are localized at the upper surface of the GDL (see Fig. 7).

3.2. Porosity and permeability fields

3.2.1. Determination of the porosity and permeability fields for half of the domain

A model of half of the GDL is created under COMSOL Multiphysics® [11]; the deformation of the GDL obtained from SAMCEF-Field software is introduced in COMSOL as a prescribed displacement, and the volumetric deformation field $e_v(x,y)$ is then calculated as follows:

$$e_v(x,y) = e_x(x,y) + e_y(x,y) + e_z(x,y) \tag{1}$$

One can easily show that the porosity field might be evaluated according to:

$$\varepsilon(x,y) = \frac{\varepsilon_0 + e_v(x,y)}{1 + e_v(x,y)} \tag{2}$$

where ε_0 is the initial GDL porosity before compression.

Finally, the local permeability K is obtained as follows [12]:

$$K(x,y) = C\frac{[\varepsilon(x,y)]^3}{[1-\varepsilon(x,y)]^2} \tag{3}$$

where C is a constant given for different materials of the GDL.

3.2.2. Determination of the complete porosity and permeability fields

Assuming symmetry with respect to the vertical X axis, the local porosity and permeability fields are extended to a complete domain with MATLAB software. Here, a regular grid covering the complete domain is created and the value of the porosity at each node is evaluated by interpolation. Moreover, the effective local diffusion coefficients that are function of porosity are then obtained according to [13] using the following expression:

$$D_{\text{eff}}(x,y) = C_D \times 10^{-4} \times \left(\frac{T}{T_{\text{ref}}}\right)^{1.5} \times \varepsilon^{1.5} \tag{4}$$

where C_D and T_{ref} are different for each couple of gas components as in Table 3.

Interpolation files are created for future use in the multi-physical model built under COMSOL Multiphysics®.

3.3. The multi-physical model of the fuel cell

The following equations govern the different phenomena in the fuel cell; the used symbols are defined in the nomenclature at the end of this paper.

In both the anode and the cathode GDLs, the potential distribution is governed by:

$$\nabla \cdot (-k_e \nabla V_e) = 0 \tag{5}$$

In the membrane, the potential distribution is governed by:

$$\nabla \cdot (-k_m \nabla V_m) = 0 \tag{6}$$

The voltage difference between the cathode and the anode corresponds to the total potential of the fuel cell.

For the GDL, transport is modeled in porous medium; the continuity equation in the GDL is given by:

$$\nabla \cdot (\rho \varepsilon u) = 0 \tag{7}$$

where the velocity field is obtained using the Darcy's law as follows:

$$u = -\frac{K}{\eta}\nabla p \tag{8}$$

Dirichlet conditions are applied for the velocity field at the anode and the cathode boundaries of the GDL; the velocities at these boundaries are obtained from the electrochemical reaction rates. At the anode side, we have:

$$-n \cdot u = \frac{i_a}{\rho F} \times \left(\frac{M_{H_2}}{2} + \text{drag}_{H_2O} \times M_{H_2O}\right) \tag{9}$$

while at the cathode side, we have:

$$-n \cdot u = \frac{i_c}{\rho F} \times \left[\frac{M_{O_2}}{4} + \left(\frac{1}{2} + \text{drag}_{H_2O}\right) \times M_{H_2O}\right] \tag{10}$$

In porous medium, the mass transport equation takes into consideration the different species according to the Maxwell–Stephan diffusion convection equation given by:

$$\nabla \cdot \left[-\rho\omega_i \sum_{j=1}^{N} D_{ij}\left\{\frac{M}{M_j}\left(\nabla\omega_j + \omega_j\frac{\nabla M}{M}\right)\right\} + \omega_i \rho u\right] = 0 \tag{11}$$

We remind the effective diffusion coefficients that are function of the porosity are given by Eq. (4).

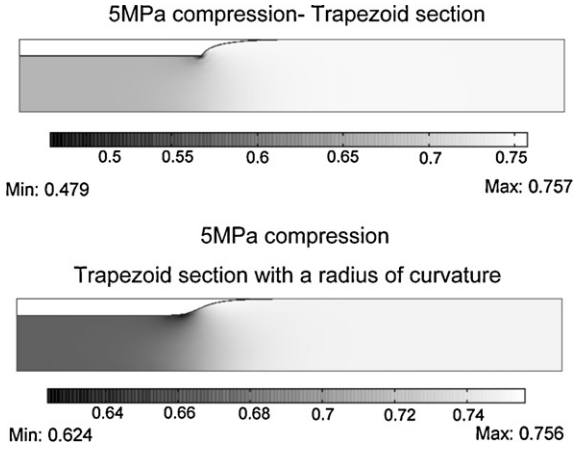

Fig. 8. Porosity fields for graphite bipolar plates.

Now, the local current density distribution in the catalyst layer (i_c) is obtained from the Butler–Volmer expression (Eq. (12)); a similar expression is also available for i_a.

$$i_c = i_{0,c}^{\text{ref}} \frac{\omega_{O_2}}{\omega_{O_{2,0}}} \exp\left(-\alpha \times \frac{F\eta_{act,c}}{RT}\right) \tag{12}$$

Navier–Stokes equations govern the assumed laminar flow inside the channels of the bipolar plates, where transport is ensured via a pressure gradient. The Navier–Stokes equations (momentum and continuity) in a porous medium are given by:

$$\rho\left(\frac{\partial u}{\partial t} + u \cdot \nabla u\right) = -\nabla p + \eta \nabla^2 u + f, \quad \nabla \cdot u = 0 \tag{13}$$

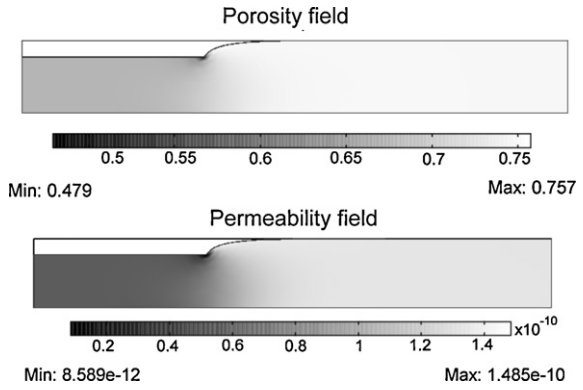

Fig. 9. Comparison of the porosity and permeability fields. Compression of a trapezoid section at 5 MPa.

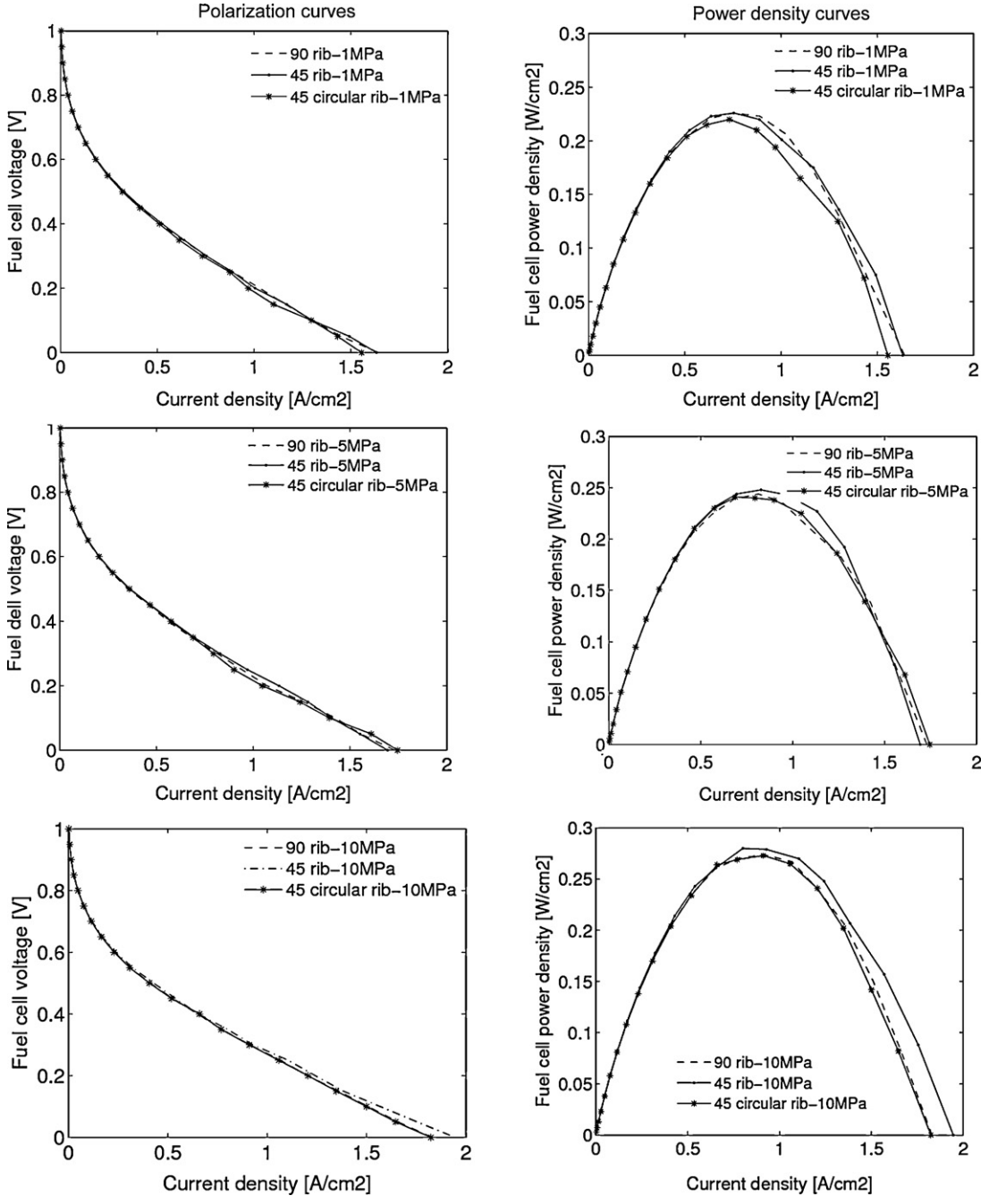

Fig. 10. Polarization and power density curves for graphite bipolar plates—influence of the geometry of the bipolar plates.

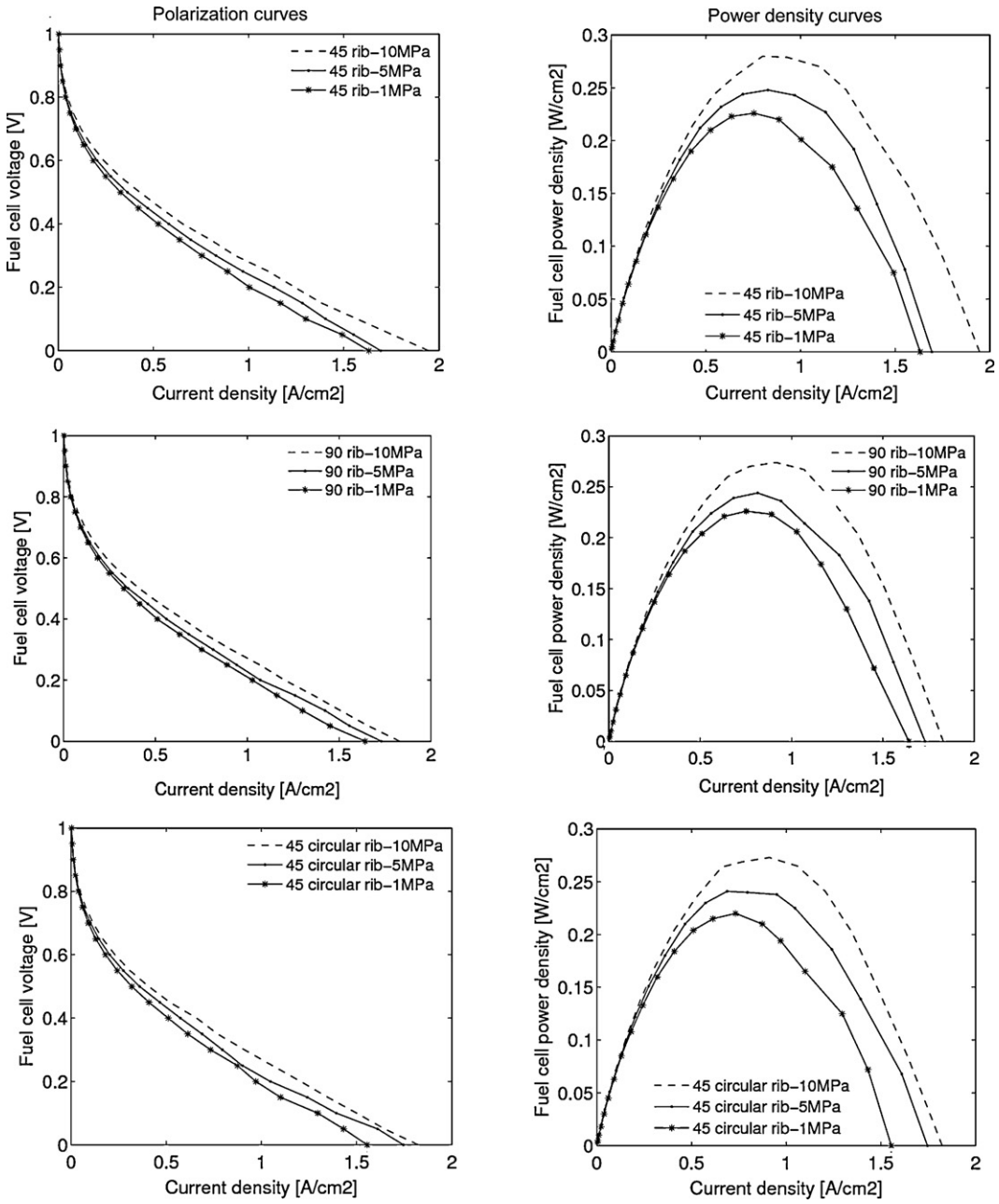

Fig. 11. Polarization and power density curves for graphite bipolar plates—influence of compression.

Finally, the different species are transported according to the classical convection-diffusion transport equation, and again Dirichlet conditions are applied at the anode and the cathode boundaries of the GDL. At the catalyst layers, the hydrogen mass-flux at the anode and the oxygen mass-flux at the cathode are given by:

$$\begin{aligned} -n \cdot N_{H_2} &= \frac{i_a}{2F} \times M_{H_2} \\ -n \cdot N_{O_2} &= \frac{i_c}{4F} \times M_{O_2} \\ -n \cdot N_{H_2O} &= \frac{i_c}{F} \times \left(\frac{1}{2} + \mathrm{drag}_{H_2O}\right) \times M_{H_2O} \end{aligned} \tag{14}$$

The PEMFC model built in COMSOL Multiphysics Chemical Engineering Module [13] consists in solving Eqs. (4)–(14) using a finite element method. For every section type of the channels and for every pressure magnitude, simulations are conducted for different values of the fuel cell potential. The local current density is computed, and the polarization and the power density curves can then be obtained. Fig. 6 shows the quality of the mesh (consisting of 1361 elements) used in the case of a trapezoid section of the channel with a 0.2 mm curvature radius and for a pressure of 5 MPa.

4. Results of the numerical analysis

We remind that the values of the electrochemical transport parameters are listed in Table 1 and that the geometric and operation parameters of the components are listed in Table 2.

4.1. Mechanical deformations

Fig. 7 shows the deformations of the bipolar plate and the GDL under a constant pressure of 10 MPa, applied on the upper boundary of the domain. This pressure, even though is higher than an expected pressure in reality, underlines the intended results which are the deformation of the GDL in contact with the bipolar plate and

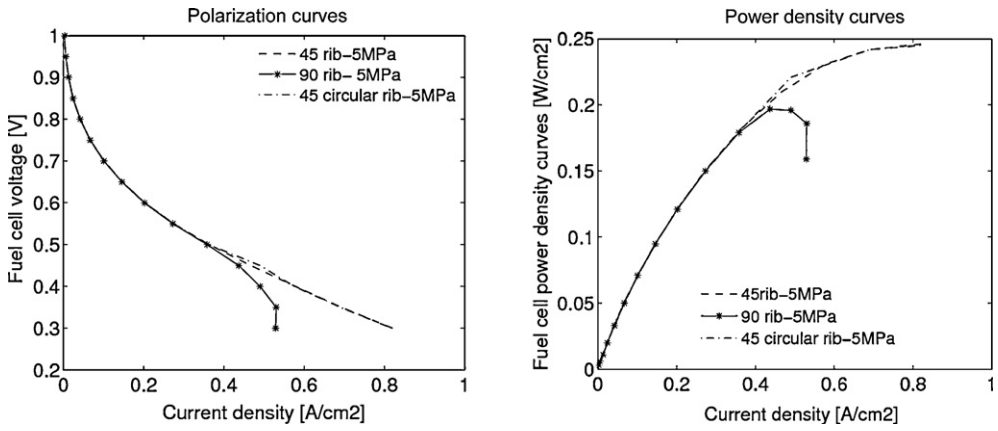

Fig. 12. Polarization and power density curves for thin steel bipolar plates.

the contact zones with this same bipolar plate (detachment points). For an applied compression force of 10 MPa, the deformation of the steel bipolar plate is much higher than that of the graphite one. On the other hand, the rectangular sections lead to a corner type pressing in the GDL where the detachment point is on the vertical. These results are transmitted to an excel sheet for the determination of the GDL deformation.

Table 4 resumes the decrease of GDL thickness under the rib as a result of the applied compression forces and of the channel sections of the graphite bipolar plates. For a pressure magnitude of 10 MPa in the case of a rectangular section of the bipolar plates, the thickness of the GDL under the rib is decreased considerably (44% approximately) whereas for a pressure magnitude of 1 MPa and for the same type of bipolar plate, the thickness of the GDL under the rib is decreased by 4% approximately.

4.2. Porosity and permeability fields

Since compression reduces locally the thickness of the GDL, its porosity varies according to the above-mentioned principles (see Section 3.2.1). Fig. 8 represents a half-rib and a half-channel from the cathode side, and shows the local porosity fields associated with a compression force of 5 MPa for two types of graphite bipolar plates (trapezoid section and trapezoid with a rounded edge); it also shows the local influence of the radius of curvature. Fig. 9 compares the local porosity and permeability fields obtained in the case of a 5 MPa compression force for a trapezoid section of the bipolar plates. As for the porosity field, the permeability field also changes locally due to an applied compression.

4.3. Polarization and power density curves

In order to isolate the influence of the local porosity and the local permeability, the polarization and the power density curves are obtained from several simulations in which the fuel cell potential varies from 0 up to 1 V with steps of 0.05 V. However, these simulations do not take into consideration the variation of the contact resistances.

Considering graphite bipolar plates, curves have been elaborated for the three different sections of ribs (rectangular, trapezoid and trapezoid with a rounded edge) and for the pressure magnitudes of 1 MPa, 5 MPa and 10 MPa. They are represented into two different ways: Fig. 10 underlines the influence of the geometry while Fig. 11 shows the influence of loadings. It can be observed that the geometric parameters (sections of the ribs of the bipolar plate) as well as the compression pressures on the fuel cell influence its performance through the local variation of the porosity and permeability fields. Fig. 10 shows the effect of the rib shape on the efficiency of the fuel cell. At high pressures (10 MPa) and for high current densities, only the shape of the trapezoid rib gives slightly a better performance; whereas at low pressures, the polarization and power density curves are very close to each other for all the considered sections (rectangular, trapezoid and trapezoid with a 0.2 mm curvature radius).

The polarization and power density curves of Fig. 11 show an improvement of the performance of the fuel cell at high pressure magnitudes; this is valid for all the sections of the graphite bipolar plate. Because of cell compression, the GDL is thinner under the rib and bends under the channel, the volume of the gas flux is then

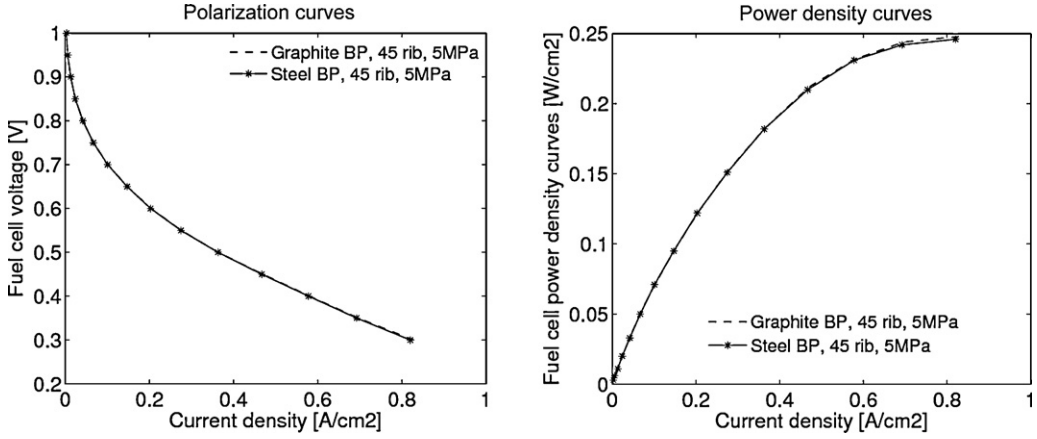

Fig. 13. Polarization and power density curves for graphite and for steel bipolar plates at 5 MPa and for a trapezoid section of the bipolar plates.

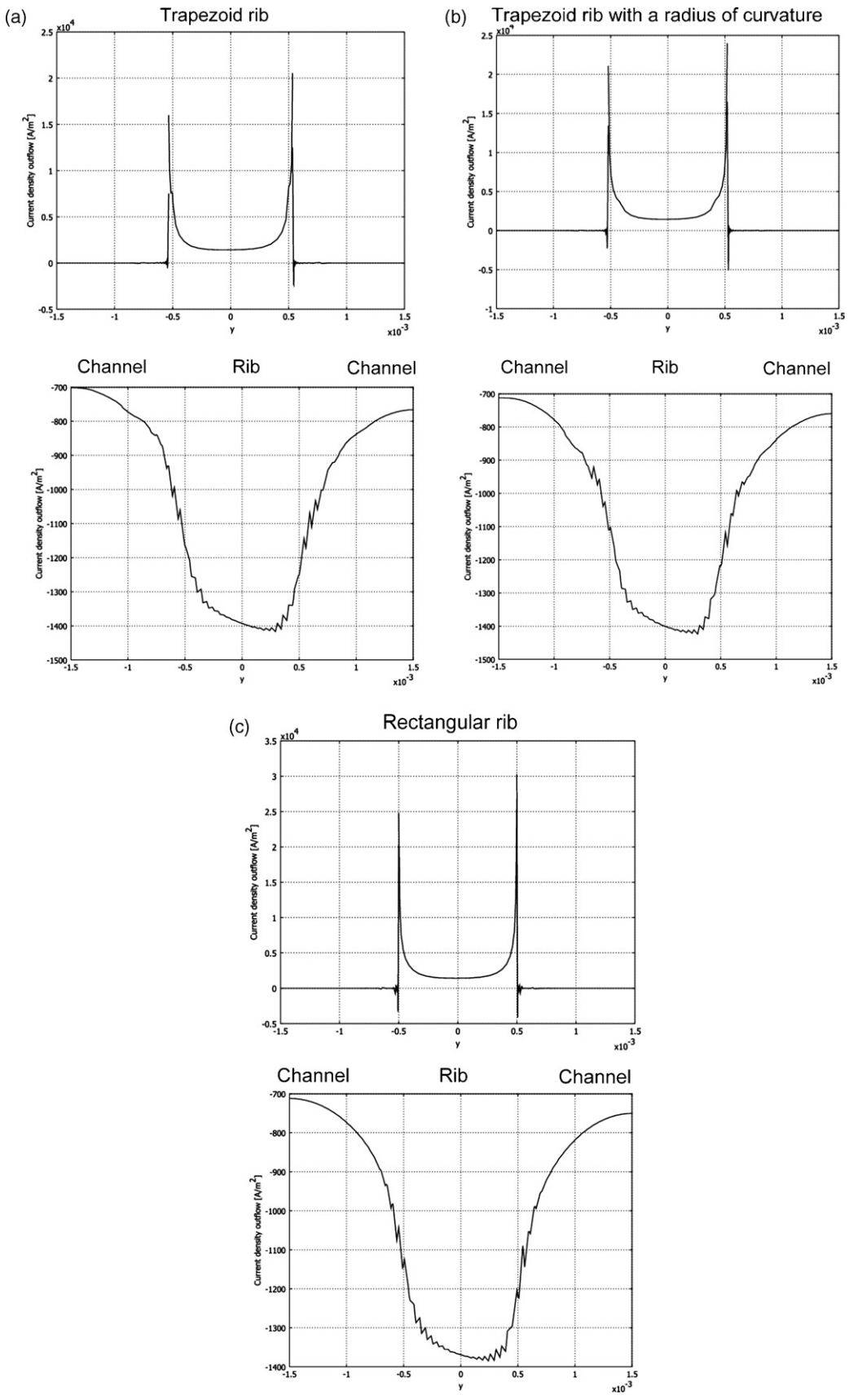

Fig. 14. Local current density – graphite ribs – compression of 5 MPa.

smaller which increases gas velocity and improves mass transfer. Moreover, fuel cell compression decreases the contact resistance between the bipolar plate and the GDL; this decreases in turn the losses and improves the performance of the cell.

The same procedure has been executed for steel bipolar plates. Fig. 12 shows the polarization and power density curves for steel bipolar plates, for three types of sections and for a load of 5 MPa. The polarization and the power density curves of the trapezoid sections (with and without a rounded edge) of the steel bipolar plates are equivalent but the rectangular section presents limits of use at high values of the current density. This loss in performance at high current densities for rectangular sections of the steel bipolar plates does not exist for the graphite bipolar ones; we suppose that this is due to the large mechanical deformations of the steel plate. This conclusion will be verified in future studies; however that may be, this confirms the choice of trapezoid section for the steel bipolar plates.

Fig. 13 shows that, for trapezoid sections of graphite and steel bipolar plates, there is no difference regarding the polarization and power density curves, at least until a compression force of 5 MPa. This is also true for trapezoid sections with rounded edges of the bipolar plates.

4.4. Local current density

For all the considered sections of the graphite bipolar plates, for a cell potential of 0.7 V, and for a pressure magnitude of 5 MPa, Fig. 14 shows the distribution of the local current densities on two interfaces:

- the interface between the GDL and the bipolar plate,
- and the interface between the GDL and the cathode.

We draw the lecturer's attention on the non-symmetric character of the local curves; this is due to the pressure gradients between the channels at the left and at the right of the rib. On the other hand, the results of the simulations show that the regions of high current densities are the most critical because of the reduction of oxygen diffusion induced by the cell compression and because we did not account for the flooding effect at the cathode. Moreover, the lower parts in Fig. 14(a)–(c) have not been smoothed; these are the raw results of the iterative process of computation that depends on the mesh size and on the applied convergence threshold.

For a rectangular rib and at 5 MPa, the detachment of the GDL occurs at the rib corner (the detachment point is the last point of contact between the uncompressed GDL and the rib); this is why current peaks appear in the upper part of Fig. 14(c) at ± 0.5 mm.

Also for a compression force of 5 MPa and for a trapezoid rib with or without a radius of curvature, the GDL stays in contact with a part of the channel side. The rib seems larger and the current peaks occur at the detachment points of the GDL on the side of the channels as shown in the upper parts of Fig. 14(a) and (b). This is how a part of the channel side plays the role of current collector and the current peaks show the effects of the inhomogeneous compression of the cell on the local current density distribution.

5. Conclusion

This paper presented different fuel-cell models in which the GDL compression is studied along with the effects of compression on fuel cell performance; typical results and specific properties of each model have also been given. The GDL porosity, the contact resistance, the permeability, and the conductivity are all influenced by mechanical solicitations and hence cannot be kept constant throughout the modeling of PEMFC. Many phenomena affect the properties of the fuel cell and influence its power production. The effects of such phenomena and their multi-physical coupling are studied in this paper and their influence on fuel cell performance has been investigated. In order to study the effects of the bipolar plate geometry and the compression forces on the performance of a fuel cell, a mechanical model for computing the GDL deformation has first been established. Then, a multi-physical model has been elaborated; this model takes into consideration the porosity and the permeability fields that vary locally in order to approach the real conditions of use of a PEMFC. Fuel cell performance has been deduced from the polarization and power density curves for different types of bipolar plates and for different pressure magnitudes. It is necessary to emphasize the fact that the permeability and the effective diffusion coefficients of our model vary locally because they are function of the porosity. Finally, we observed current peaks that might affect the local current distribution and the temperature distribution inside the cell. Modeling of a fuel cell system needs further analysis, such as modeling the electrodes and taking into consideration the energy equation among the governing equations a fuel cell system, in order to approach the real conditions of use of the cell. Note that we took into consideration the deformation of the bipolar plates in the applied method. Among the two types of material and the three types of sections that have been considered, only the steel bipolar plates are deformed visibly. However, this deformation does not have an impact on the polarization curves, despite the fact that there is a little local effect on the GDL compression. Other effects might also interfere and should therefore be deepened; mainly, the electrodes modeling and the heat transfer might influence the behavior of the fuel cell and, particularly, its performance.

References

[1] P. Zhou, C.W. Wu, G.J. Ma, J. Power Sources 159 (2006) 1115–1122.
[2] P. Zhou, C.W. Wu, G.J. Ma, J. Power Sources 163 (2007) 874–881.
[3] Y. Zhou, G. Lin, A.J. Shih, S.J. Hu, J. Fuel Cell Sci. Technol. 6 (4) (2009), 041005 (7 pages).
[4] L. Zhang, Y. Liu, H. Song, S. Wang, Y. Zhou, S. Jack Hu, J. Power Sources 162 (2006) 1165–1171.
[5] I. Nitta, T. Hottinen, O. Himanen, M. Mikkola, J. Power Sources 171 (2006) 26–36.
[6] N. Fekrazad, T.L. Bergman, J. Heat Transfer 129 (2007) 1004–1013.
[7] T. Hottinen, O. Himanen, S. Karvonen, I. Nitta, J. Power Sources 171 (2007) 113–121.
[8] W. Sun, B.A. Peppley, K. Karan, J. Power Sources 144 (2005) 42–53.
[9] M. Sadiq Al-Baghdadi, H. Shahad Al-Janabi, J. Renew. Energy 32 (2007) 1077–1101.
[10] M. Sadiq Al-Baghdadi, J. Renew. Energy 34 (3) (2009) 674–682.
[11] Comsol Multiphysics, Version 3.5a.
[12] J.P. Feser, A.K. Prasad, S.G. Advani, J. Power Sources 162 (2006) 1226–1231.
[13] Comsol Multiphysics, Version 3.5a. Electrochemical Engineering: The Proton Exchange Membrane Fuel Cell.